

## POINT-PLANE DISTANCE AS MODEL FOR UNCERTAINTY EVALUATION OF COORDINATE MEASUREMENT

Wojciech Płowucha

University of Bielsko-Biala, Willowa 2, PL43-309 Bielsko-Biala, Poland  
(✉ [wplowucha@ath.bielsko.pl](mailto:wplowucha@ath.bielsko.pl), +48 338 279 321)

### Abstract

The paper presents a detailed theoretical background for coordinate measurement uncertainty evaluation by means of Type B evaluation method, taking into account information on accuracy of a coordinate measuring system given with the formula for maximum permissible errors of length measurement and verification test results. A proposal for evaluation of the verification test results is made. A measurement model based on the point-plane distance equation is presented. A detailed analysis of the partial derivatives (sensitivity factors in an uncertainty budget) of the measurement model is presented. The analyses of measurement uncertainty for different geometrical characteristics were conducted using this measurement model. Examples of uncertainty evaluation for geometrical deviations are presented: position of a point related to a datum plane and flatness in the case of convex or concave surfaces. The examples include detailed uncertainty budgets.

Keywords: task specific uncertainty, uncertainty of coordinate measurement, measurement models, Type B evaluation, sensitivity analysis method.

© 2020 Polish Academy of Sciences. All rights reserved

## 1. Introduction

Technical specification ISO/TS 15530-1 [1] distinguishes three methods of estimating uncertainty: sensitivity analysis, use of calibrated workpieces or standards and use of computer simulation. This classification diverges from the one used in *Guide to the Expression of Uncertainty in Measurement* (GUM), where the first two stages of the process of estimating uncertainty are defined: formulation and calculation, the latter being divided into propagation and summarizing [2]. Only for the propagation stage there are three possibilities: the GUM uncertainty framework, analytic methods and a Monte Carlo method. Without going into details, the sensitivity analysis is practically the GUM uncertainty framework while computer simulation is a Monte Carlo method. It is worth noting that in the GUM there is no equivalent to the “use of a calibrated object” method, and ISO 15530-1 does not mention of the possibility of an analytical approach.

The most objective method of estimating the uncertainty of coordinate measurements is the method using a calibrated object (artefact), in the form of the object being measured, provided that

the procedure was correctly used [3, 4]. In this method, almost whole uncertainty is determined experimentally. For proper use of the method, dimensional stability and high similarity of the calibrated object are important, especially in terms of the coefficient of thermal expansion. It is also important to properly design and conduct the experiment to randomize disturbing factors.

With regard to simulation methods, it should be borne in mind that the quality of simulation results depends on the quality of the *coordinate measuring machine* (CMM) errors data used. However, the most important limitation of the use of simulation software results from the time-consuming implementation procedure followed by periodic updating of input information [5]. In the context of this publication, attention should be paid to the “simulation by constraint” method [6], due to the fact that the input information there, is a formula for  $MPE(E)$ .

The method presented in VDI/VDE 2617-11 [7], based on the work of Pressel [8] and Hernla [9], can be considered as a method of sensitivity analysis. The relationships between some of the machine’s geometrical errors (perpendicularity, straightness) and the parameters of the formula for the maximum permissible length measurement error  $MPE(E)$  are shown there. Measurement models and sample uncertainty budgets for size and distance are given. However, the document does not contain complete measurement models for geometric deviations and is difficult to use because it requires understanding the significance of each uncertainty contributor [10].

The use of information contained in the formulae for  $MPE(E)$  and  $MPE(P)$  has also been proposed by Cheng [11]. The proposed approach was named the quantitative statistical analysis method. It was considered that from the point of view of uncertainty of coordinate measurements, three types of characteristics should be assessed differently: dimensions, form deviations, and orientation and location deviations. It was indicated which elements of the  $MPE(E)$  or  $MPE(P)$  formulae should be used to estimate the uncertainty in individual cases. Repeatability and reproducibility were indicated as additional two components of measurement uncertainty (an experimental method for obtaining them was proposed). Separate analyses were made for the dimension, form, two orientation deviations and two location deviations. The presented proposal is very similar to Pressel *et al.* and Hernla’s [8, 9].

In [12, 13] it has been shown that the basic condition for correct assessment of the measurement uncertainty component derived from CMM is to treat the coordinate measurement as an indirect measurement with the following conditions: the measured characteristics (dimensions, geometric deviations) should be expressed as a function of differences of coordinates of selected points corresponding to the measurement strategy based on the minimum mathematical number of points. When using the minimum number of points in the model, there is no need for including correlation, and thanks to using differences in point coordinates (instead of point coordinates), measurement traceability is ensured (compliance of the measurement model with the calibration procedure).

The problem of estimation of task specific uncertainty, especially in industrial conditions, is still up-to-date and investigated by many research centres [14–17].

## 2. Measurement model

The paper continues the concepts introduced in [18] where the point-straight line distance formula was used as the measurement model for uncertainty evaluation but the point-plane distance formula is used as the measurement model. Similarly, in this paper all geometrical characteristics (dimensions and deviations of form, orientation, location and runout) will be expressed as functions of coordinate differences of characteristic points where the characteristic

points are appropriately selected points of integral features (surfaces) or derived features (e.g. the symmetry plane)

$$l = f(x_i), \tag{1}$$

where  $l$  – geometrical characteristic,  $x_i$  – coordinates' differences of particular pairs of characteristic points.

Consequently, the combined standard uncertainty of measurement  $u_c$  will be calculated as

$$u_c = \sqrt{\sum_{i=1}^n \left( \frac{\partial l}{\partial x_i} u_{x_i} \right)^2}, \tag{2}$$

where:  $x_i$  – differences of coordinates of particular pairs of points occurring in the measurement model,  $u_{x_i}$  – measurement uncertainty of particular differences of coordinates of particular pairs of points.

The general formula for calculating distance  $l$  between point  $S$  and plane  $p$  defined by point  $P$  and the unit normal vector  $\mathbf{v}$  is

$$l(S, p) = |(\mathbf{P} - \mathbf{S}) \cdot \mathbf{v}|. \tag{3}$$

In the following, plane  $p$  is represented by three points (Fig. 1).

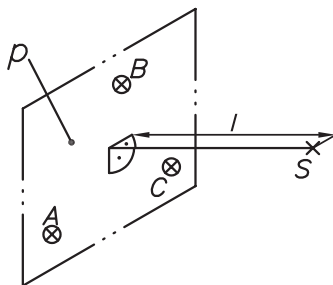


Fig. 1. Distance between the point and the plane defined by three points.

If the plane  $p$  is represented by points  $A$ ,  $B$  and  $C$  then the unit normal vector  $\mathbf{v}$  can be defined in three ways (it turns out that it matters):

$$\mathbf{v} = \frac{\mathbf{AB} \times \mathbf{AC}}{|\mathbf{AB} \times \mathbf{AC}|} \quad \text{or} \quad \mathbf{v} = \frac{\mathbf{BA} \times \mathbf{BC}}{|\mathbf{BA} \times \mathbf{BC}|} \quad \text{or} \quad \mathbf{v} = \frac{\mathbf{CA} \times \mathbf{CB}}{|\mathbf{CA} \times \mathbf{CB}|}. \tag{4}$$

Point  $A$ ,  $B$  or  $C$  can be assumed as point  $P$  in the formula (3) thus there are nine variants of the measurement model and each of them can be used for uncertainty evaluation. If the results of particular variants differ, it is justified to choose the smallest value:

$$u_c = \min(u_{c_j}), \quad j = 1, \dots, 9. \tag{5}$$

The measurement model for variant 1 is

$$l(AS, \mathbf{AB}, \mathbf{AC}) = \left| AS \cdot \frac{\mathbf{AB} \times \mathbf{AC}}{|\mathbf{AB} \times \mathbf{AC}|} \right|. \tag{6}$$

The derived formula for the distance  $l$  (measurement model) is:

$$l(a_{s1}, a_{s2}, a_{s3}, ab_1, ab_2, ab_3, ac_1, ac_2, ac_3) = \frac{a_{s1}L_1 + a_{s2}L_2 + a_{s3}L_3}{M}, \quad (7)$$

where

$$L_1 = ab_2ac_3 - ab_3ac_2, \quad (8)$$

$$L_2 = ab_3ac_1 - ab_1ac_3, \quad (9)$$

$$L_3 = ab_1ac_2 - ab_2ac_1, \quad (10)$$

$$M = \sqrt{L_1^2 + L_2^2 + L_3^2}. \quad (11)$$

The distance  $l$  is a function of nine differences of coordinates (components of vectors  $AB$ ,  $AC$  and  $AS$ ), thus the combined measurement uncertainty is geometrical sum of nine elements:

$$u_{c1} = \sqrt{\sum_{i=1}^9 \left( \frac{\partial l}{\partial x_i} u_{x_i} \right)^2}. \quad (12)$$

The derivatives present in the formula are weights (sensitivity coefficients), with which the measurement uncertainties of individual distances affect the measurement uncertainty of the measured characteristics. The respective derivatives  $\frac{\partial l}{\partial x_i}$  are:

$$\frac{\partial l}{\partial a_{s1}} = \frac{L_1}{M}, \quad (13)$$

$$\frac{\partial l}{\partial a_{s2}} = \frac{L_2}{M}, \quad (14)$$

$$\frac{\partial l}{\partial a_{s3}} = \frac{L_3}{M}, \quad (15)$$

$$\frac{\partial l}{\partial ab_1} = \frac{(-a_{s1}L_1 - a_{s2}L_2 - a_{s3}L_3)(ac_3L_2 + ac_2L_3)}{M^3} + \frac{a_{s3}ac_2 - a_{s2}ac_3}{M}, \quad (16)$$

$$\frac{\partial l}{\partial ab_2} = \frac{(-a_{s1}L_1 - a_{s2}L_2 - a_{s3}L_3)(ac_3L_1 - ac_1L_3)}{M^3} + \frac{a_{s1}ac_3 - a_{s3}ac_1}{M}, \quad (17)$$

$$\frac{\partial l}{\partial ab_3} = \frac{(-a_{s1}L_1 - a_{s2}L_2 - a_{s3}L_3)(ac_1L_2 - ac_2L_1)}{M^3} + \frac{a_{s2}ac_1 - a_{s1}ac_2}{M}, \quad (18)$$

$$\frac{\partial l}{\partial ac_1} = \frac{(-a_{s1}L_1 - a_{s2}L_2 - a_{s3}L_3)(ab_3L_2 - ab_2L_3)}{M^3} + \frac{a_{s2}ab_3 - a_{s3}ab_2}{M}, \quad (19)$$

$$\frac{\partial l}{\partial ac_2} = \frac{(-a_{s1}L_1 - a_{s2}L_2 - a_{s3}L_3)(ab_1L_3 - ab_3L_1)}{M^3} + \frac{a_{s3}ab_1 - a_{s1}ab_3}{M}, \quad (20)$$

$$\frac{\partial l}{\partial ac_3} = \frac{(-a_{s1}L_1 - a_{s2}L_2 - a_{s3}L_3)(ab_2L_1 - ab_1L_2)}{M^3} + \frac{a_{s1}ab_2 - a_{s2}ab_1}{M}. \quad (21)$$

Respectively the component uncertainties  $u_{x_i}$  are:  $u_{as1}$ ,  $u_{as2}$ ,  $u_{as3}$ ,  $u_{ab1}$ ,  $u_{ab2}$ ,  $u_{ab3}$ ,  $u_{ac1}$ ,  $u_{ac2}$ ,  $u_{ac3}$ .

It will be found that in some of the analysed cases the values of derivatives are constant for different values of the coordinates of point  $S$ . For the purpose of this publication, the values of the derivatives are presented in the form of colour surface plots. For the purpose of analysis, usually no specific derivative values are needed, and only the nature of the dependence is important, therefore no legend is placed next to the plots. If necessary, plots of the derivatives values in the selected cross-sections are placed next to the surface plot.

The further illustration consider the example in which the datum plane is a square with the side slightly larger than 300 mm. The characteristic points, defining the plane, are distributed on the edges of the square with the side equal to 300 mm. The tolerated element is located 200 mm away from the datum. The analysis of the measurement uncertainty is carried out for various positions of point  $S$  (toleranced feature) in a square-shaped area with a side of 400 mm. All analyses are performed for the workpiece oriented along the axes of the coordinate system i.e. points  $A$ ,  $B$  and  $C$  lay in the same plane of the coordinate system.

In the discussed variant for any location of point  $S$  six partial derivatives  $\frac{\partial l}{\partial as_1}$ ,  $\frac{\partial l}{\partial as_2}$ ,  $\frac{\partial l}{\partial ab_1}$ ,  $\frac{\partial l}{\partial ab_2}$ ,  $\frac{\partial l}{\partial ac_1}$ ,  $\frac{\partial l}{\partial ac_2}$  equal 0 and one derivative  $\frac{\partial l}{\partial as_3}$  equals 1. The values of the remaining two derivatives  $\frac{\partial l}{\partial ab_3}$ ,  $\frac{\partial l}{\partial ac_3}$  depend on the location of point  $S$ . The plots of  $\frac{\partial l}{\partial ab_3}$  are presented in Fig. 2.

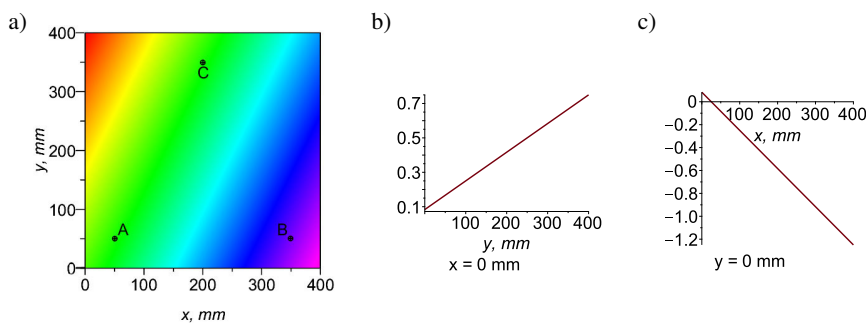


Fig. 2. Plots of derivative  $\frac{\partial l}{\partial ab_3}$  in function of location of point  $S$ : a) surface plot, b) plot of cross-section  $x = 0$  mm, c) plot of cross-section  $y = 0$  mm.

The presented plots show that the derivative  $\frac{\partial l}{\partial ab_3}$  has constant values on the lines parallel to the line  $AC$ . The derivative over the analysed area changes its value in the range from  $-1.25$  to  $0.75$ . The value of the derivative over points  $A$ ,  $B$ ,  $C$  equals respectively:  $0$ ,  $-1$ ,  $0$ .

The plots of the derivative  $\frac{\partial l}{\partial ac_3}$  are presented in Fig. 3.

The presented plot shows that the derivative  $\frac{\partial l}{\partial ac_3}$  has constant values on the lines parallel to the line  $AB$ . The derivative over the analysed area changes its value in the range from  $-1.17$  to  $0.17$ . The value of the derivative over points  $A$ ,  $B$ ,  $C$  equals respectively:  $0$ ,  $0$ ,  $-1$ .

Similar calculations should be made for the remaining eight variants. The results of these calculations will be used in uncertainty budgets for specific characteristics based on this model.

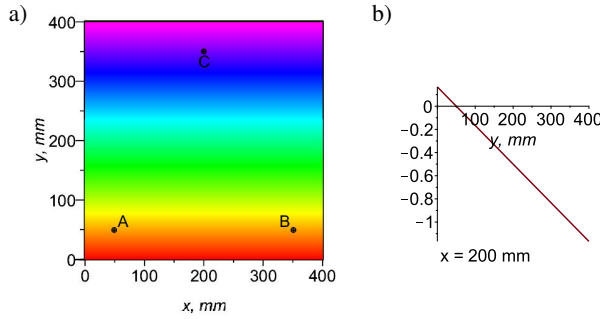


Fig. 3. Plots of the derivative  $\frac{\partial l}{\partial ac_3}$  in function of location of point  $S$ :  
 a) surface plot, b) plot of cross-section  $x = 0$  mm.

### 3. Evaluating information on CMM accuracy

In its basic version, the GUM approach assumes that the measurement model is known (the function that links input quantities to the output quantity on the basis of which it is possible to determine the sensitivity coefficients) and that standard uncertainties for all input quantities are known or estimable. When the conditions of the central limit theorem are met, the combined uncertainty of measurement is calculated as a geometric sum of component uncertainties (products of the standard uncertainty of input quantities and sensitivity factors). The calculations are documented in the form of an uncertainty budget.

In cases where input information is in the form of a series of observations, the uncertainties of individual input quantities are calculated as standard deviation from the recorded observations (method A), and in cases where the information about the input quantity is a probability distribution, it is converted into standard deviation (method B). In the second case, most often symmetrical distributions of a simple form are used (*e.g.* uniform, U, bimodal) defined by means of maximum error values.

The GUM approach generally does not use asymmetrical distributions and in justified cases the so-called symmetrisation is used. A typical example of symmetrisation for method B is replacement of systematic errors with a bimodal distribution [7], while in the case of method A it is replacement of standard deviation with a second moment relative to zero [19, p. 1.14].

In coordinate measurements, CMM and environmental conditions are the main determining factor of measurement accuracy. Information on CMM accuracy is usually presented as a linear function expressing the maximum permissible error of length measurement in function of the measured length  $L$ :  $MPE(E) = \pm A + BL/1000$  or  $MPE(E) = \pm(A + L/K)$ . This formula covers the influence of environmental conditions within the range specified by the manufacturer. The accuracy of the CMM is verified by calibration (verification tests).

The CMM calibration results are usually 105 length measurement errors of several material length standards [20]. Depending on technical conditions and actual environmental conditions of CMM usage, the error diagram (calibration results) uses a smaller or larger  $MPE(E)$  range.

In order to take into account the state of CMM for estimating uncertainty, the author proposes to calculate the standard uncertainty of length measurement using the formula for  $MPE(E)$  and an appropriate factor  $\lambda$ , *i.e.* writing the formula for the standard uncertainty of length measurement  $u_{CMM}$  in the form

$$u_{CMM} = \frac{MPE}{\lambda} \quad (22)$$

The coefficient  $b = 1/\lambda$  (in case of uniform distribution  $\lambda$  equals to  $\sqrt{3}$ ) will be calculated on the basis of the calibration results as the square root of the second sample moment about zero from standardized error values (range  $(-1, 1)$ ):

$$b = \frac{1}{\lambda} = \sqrt{\frac{1}{105} \sum_{i=1}^{105} E_{si}^2}, \quad (23)$$

where  $E_{si}$  are the values of  $E_i$  errors standardized according to the formula

$$E_{si} = \frac{E_i}{MPE(E_i)}, \quad i = 1, \dots, 105. \quad (24)$$

The presented proposal is a generalization of the approach from [21, p. 8.4.5] to the situation in which  $MPE(E)$  is not a constant value but a function of the measured length, and that the parameter  $\lambda$  which will be calculated by Type A evaluation method. In the absence of information on the nature of probability distribution of errors (when no CMM calibration certificate is available), assuming uniform distribution, standard uncertainty can be calculated with Type B evaluation as

$$u_{\text{CMM}} = \frac{MPE}{\sqrt{3}}. \quad (25)$$

An example of a CMM errors diagram with plots of normal probability density functions is presented in Fig. 4. The plots were drawn in the  $\pm 2u_{\text{CMM}}$  range to show the essence of the proposed approach (outside the  $\pm 2u_{\text{CMM}}$  area, 5% of errors can be expected). For the example shown  $\lambda = 2.55$ .

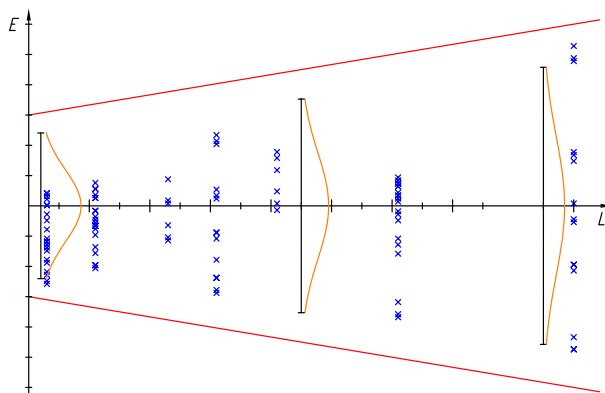


Fig. 4. Sample diagram of length measurement errors with plots of normal distribution density functions in the range  $\pm 2u_{\text{CMM}}$ .

In order to obtain comparability of results with those presented in [18], in the examples below it was assumed that  $\lambda = 3$  and the formula for the maximum permissible error of length measurement  $MPE(E)$  is

$$MPE(E) = \pm (2 + 4L/1000) \mu\text{m}. \quad (26)$$

#### 4. Uncertainty of measurement of a point position related to a datum plane

Figure 5 presents an example of a measurement model of point (centre of a ball) position related to a datum plane.

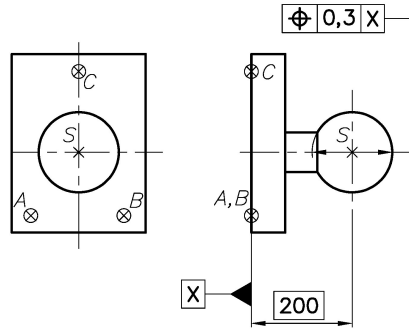


Fig. 5. Sample diagram of length measurement errors with plots of normal distribution density functions in the range  $\pm 2u_{CMM}$ .

The tolerance zone according to ISO 1101 is limited by a pair of planes parallel to the datum plane and equidistant from the point position defined by theoretically exact dimension (TED). The position deviation  $POS_{PT}$  is the smallest distance between the mentioned pair of planes covering the relevant actual point, *i.e.* doubled value of distance  $l$  of point  $S$  from the plane distant from the datum by the value of the theoretically exact dimension  $l_{TED}$ :

$$POS_{PT} = 2(l - l_{TED}). \quad (27)$$

The standard uncertainty of point position measurement  $u_{POS_{PT}}$  is therefore equal to twice the uncertainty of measurement of the distance of a point from plane  $u_l$ .

$$u_{POS_{PT}} = 2 \cdot u_l. \quad (28)$$

The uncertainty of position deviation measurement may depend on the location of point  $S$  in relation to the datum.

In the following an example of a workpiece is presented in which the datum plane is a square with a side length of 300 mm and the toleranced element is located 200 mm from the datum. Evaluation of the measurement uncertainty is carried out for characteristic points:  $A(50, 50, 10)$ ,  $B(350, 50, 10)$ ,  $C(200, 350, 10)$ ,  $S(200, 50, 210)$ .

The calculated standard uncertainties of measurement of distance between the point and the plane for the variants 1–3 as the function of coordinates  $x, y$  (within the range of the datum plane extent) of point  $S$  are presented in Fig. 6.

The uncertainty values vary over the analysed area from ca.  $0.93 \mu\text{m}$  to  $1.05 \mu\text{m}$ . The smallest values occur over points  $A, B, C$  and are  $0.93 \mu\text{m}$ .

The final result of measurement uncertainty calculated with formula (5) is presented in Fig. 7.

It can be seen in the figures above that the uncertainty values depend on the location of point  $S$ , but the differences over the analysed area are not large. For the presented example (the datum plane is a square with a side of 300 mm, the toleranced element is 200 mm away from the datum) the values of complex uncertainty are in the range from  $0.93$  to  $0.99 \mu\text{m}$ .



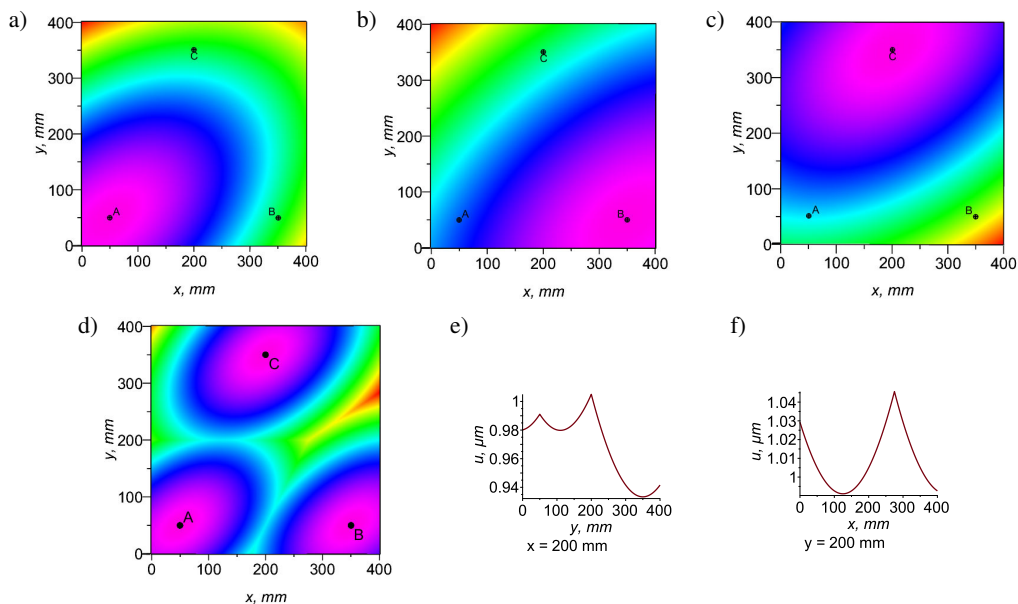


Fig. 6. The combined standard uncertainty of measurement of distance between a point and a plane: a) variant 1 ( $AS AB AC$ ), b) variant 2 ( $BS AB AC$ ), c) variant 3 ( $CS AB AC$ ), d) minimum from variants 1–3, e) plot of section  $x = 200$  mm, f) plot of section  $y = 200$  mm.

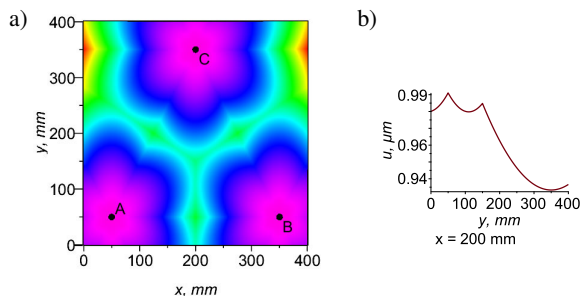


Fig. 7. The final result of calculated combined standard uncertainty of measurement of distance between a point and a plane: a) minimum from variants 1–9, b) plot of section  $x = 200$  mm.

The obtained results allow to analyse the problem of dependence of measurement uncertainty on coordinates  $x$ ,  $y$  of the sphere centre. It can be seen that the uncertainty of measurement is the smallest if the centre of the ball lies above one of the characteristic points and increases as it moves away from this point (Fig. 7b, section  $x = 200$  mm).

The graphs shown in Fig. 7 indicate that the measurement uncertainty of the position of a point depends (although only to a small extent) on the location of the centre of the ball relative to the datum edges. The extent to which uncertainty depends on the distance of the tolerated element from the datum can be seen in the uncertainty budget (Tables 1 and 2).

The uncertainty budgets for the measurement of the distance of a point from a plane, for point  $S$  with coordinates (200, 350, 210) and (200, 50, 210) corresponding to the extreme values of combined standard uncertainty, are given in Tables 1 and 2 respectively.

The uncertainty budget in Table 1 shows that in the case of point *S* being located over the characteristic point of the datum feature only one non-zero component occurs in the budget with weight factor equal 1 corresponding to the distance of point *S* from the datum plane.

Table 1. Uncertainty budget for point *S*(200, 350, 210).

Component	$x_i$ , mm	$\frac{\partial l}{\partial x_i}$	$u_{x_i}$ , $\mu\text{m}$	$\frac{\partial l}{\partial x_i} u_{x_i}$ , $\mu\text{m}$
<i>cs</i> <sub>1</sub>	0	0	0.67	0
<i>cs</i> <sub>2</sub>	0	0	0.67	0
<i>cs</i> <sub>3</sub>	200	1	0.93	0.93
<i>ca</i> <sub>1</sub>	150	0	0.87	0
<i>ca</i> <sub>2</sub>	300	0	1.07	0
<i>ca</i> <sub>3</sub>	0	0	0.67	0
<i>cb</i> <sub>1</sub>	-150	0	0.87	0
<i>cb</i> <sub>2</sub>	300	0	1.07	0
<i>cb</i> <sub>3</sub>	0	0	0.67	0
			<i>u</i> =	0.93

In the uncertainty budget for the location of point *S* corresponding to the largest value of the combined uncertainty (Table 2) there are 2 non-zero components. One of the components, with a weight of 1, corresponds to the distance of point *S* from the datum plane. The second non-zero uncertainty component, corresponding to the difference of *z* coordinates of the characteristic points of the datum plane, occurs in the budget with the weight factor of 0.5, which corresponds to the proportion of component of distance of point *S* from the datum plane edge (*as*<sub>1</sub> = 150 mm) to the width of the datum (*ab*<sub>1</sub> = 300 mm).

Table 2. Uncertainty budget for point *S*(200, 50, 210) (only non-zero elements are shown).

Component	$x_i$ , mm	$\frac{\partial l}{\partial x_i}$	$u_{x_i}$ , $\mu\text{m}$	$\frac{\partial l}{\partial x_i} u_{x_i}$ , $\mu\text{m}$
<i>as</i> <sub>3</sub>	200	1	0.93	0.93
<i>ab</i> <sub>3</sub>	0	-0.5	0.67	0.33
			<i>u</i> =	0.99

In order to analyse how the measurement uncertainty is affected by the dimensions of the datum, the calculations were repeated for cases when its dimensions are smaller (side length 50 mm) and larger (side length 500 mm). The resulting uncertainty remained the same, *u* = 0.99  $\mu\text{m}$ .

The influence of the distance of point *S* from the datum was also analysed. The dependence of the measurement uncertainty of position deviation on the distance of the toleranced feature from the datum, for distances in the range (0-500) mm, is shown in Fig. 8.

The dependence is not exactly but practically linear because, as follows from the analyses above, it is the geometric sum of two components: one component linearly increasing with change of the distance between the point and the datum and a constant component of a significantly smaller value.

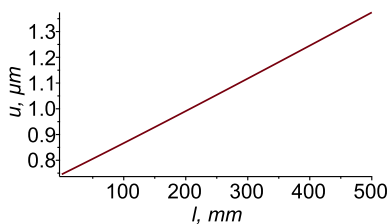


Fig. 8. The uncertainty of measurement of distance between a point and a plane.

The analyses above are valid also for the position of the axis and the position of the plane in regard to the datum plane.

### 5. Uncertainty of flatness measurement

Fig. 9 depicts the measurement model of flatness in case of convex or concave flatness deviation.

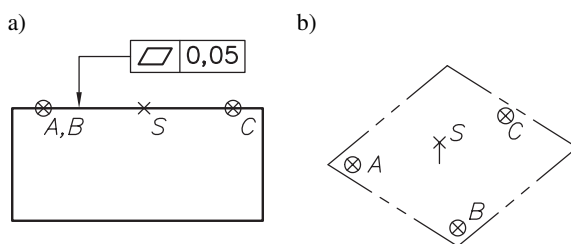


Fig. 9. Example of a specification and measurement model of flatness deviation: a) example of specification with characteristic points, b) model for uncertainty evaluation.

The tolerance zone according to ISO 1101 is limited by a pair of parallel planes. The flatness deviation  $FLT$  is the smallest distance between the mentioned pair of planes covering all the actual points of the tolerated plane, i.e. value of distance  $l$  of point  $S$  from plane  $ABC$ :

$$FLT = l. \tag{29}$$

The standard uncertainty of flatness measurement  $u_{FLT}$  is therefore equal to the uncertainty of measurement of the distance of a point from plane  $u_l$ .

$$u_{FLT} = u_l. \tag{30}$$

In reference to the example presented in Fig. 9, it should be noted that the largest value from the extent of the tolerated plane should be taken as the uncertainty of measurement of flatness deviation.

Below an example is analysed of a workpiece in which the tolerated plane is a square with a side size of 300 mm. The distribution of points of plane  $ABC$  is identical to the example concerning position of the point in regard to the plane (Fig. 7), i.e.:  $A(50, 50, 10)$ ,  $B(350, 50, 10)$ ,  $C(200, 350, 10)$ . The nature of the plot of the combined measurement uncertainty, for any values

of coordinate  $y$  of point  $S$  (Fig. 10b), is identical to that shown in Fig. 7b (section  $x = 200$  mm). The uncertainty budget for the location of point  $S(200, 50, 10.01)$  which corresponds to the largest uncertainty value is presented in Table 3.

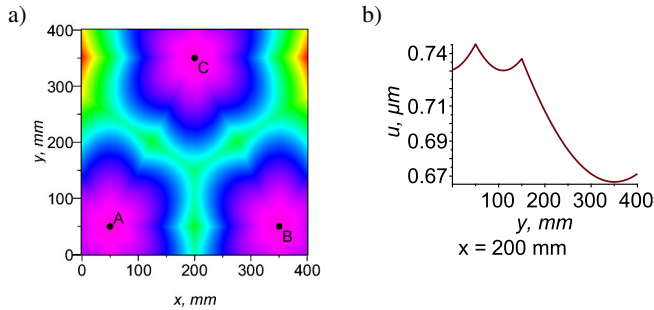


Fig. 10. The combined measurement uncertainty of distance between a point and a plane: a) surface plot, b) plot of section  $x = 200$  mm.

Table 3. The uncertainty budget for point  $S(200, 50, 10.01)$  (only non-zero components are shown).

Component	$x_i, \text{mm}$	$\frac{\partial l}{\partial x_i}$	$u_{x_i}, \mu\text{m}$	$\frac{\partial l}{\partial x_i} u_{x_i}, \mu\text{m}$
$as_3$	0.01	1.00	0.67	0.67
$ab_3$	0	-0.5	0.67	0.33
			$u =$	0.99

In the uncertainty budget for the location of point  $S$  corresponding to the largest value of the combined uncertainty (Table 3) there are 2 non-zero components. The first component, with a weight factor of 1, corresponds to the distance of point  $S$  from the datum plane ( $as_3$ ). The second non-zero uncertainty component, corresponding to the coordinate difference from the characteristic points of the plane ( $ab_3$ ), appears in the budget with a weight factor of 0.5, which corresponds to proportion of component of the distance of point  $S$  from the edge of the plane ( $as_1 = 150$  mm) to the width of the plane ( $ab_1 = 300$  mm).

## 6. Conclusions

The presented simple model of measurement (distance between a point and a plane defined by 3 points) enables uncertainty evaluation for different measuring tasks. In addition to the discussed cases of position and flatness deviations the same model can be applied for uncertainty evaluation of out-of-plane parallelism of axes.

The fact that in uncertainty budgets including nine components only two or three have values different from zero results from the assumed orientation of the workpieces according to the axes of the CMM coordinate system. Otherwise, more non-zero components occur in the uncertainty budget, but the combined uncertainty is virtually the same.

Assuming orientation of the workpiece along the CMM coordinate system axes enables to observe the principle of the uncertainty propagation, *i.e.* what weights values have particular uncertainty components in different measuring tasks.

In the presented examples the largest component that occurs in the uncertainty budget corresponds to the measurand which, in the case of position, is the value of the distance between the tolerated feature and the datum plane and, in the case of flatness, it is the value of the deviation. This component always has its weight value equal to 1. In the case of position, the value of this uncertainty component increases with the increasing distance according to the formula for the maximum permissible error of length measurement.

To estimate the uncertainty of all measurement tasks a significant number of more complex models is needed. The models are based not only on the point-plane distance but also on other models such as point-straight line, point-point, straight line-straight line as well as others.

The presented method, thanks to the use of calibration results, takes into account the technical state of the CMM and environmental conditions in which it works. It is worth mentioning that CMM manufacturers often specify different *MPE (E)* formulae for different ranges of temperature conditions. In this case proper corresponding formulae should be used in the evaluation.

Comparing to the method described in ISO 15530-3, the presented approach is more practical, especially for industrial conditions, because it does not require a calibrated artefact and a relatively laborious experiment.

Each new method should be verified. For this purpose, one can use artefacts of a simple form *e.g.* a cylinder square, ring gauges, flatness standards or specially designed artefacts such as Multi-Feature-Check [22]. The preliminary evaluation experiments for the presented method were carried out with the use of a cylinder square. Currently, extensive experimental research is carried out in several research centres across Europe within the EMPIR EURAMET-founded joint research project no. 17NRM03 in which the author takes part.

## Acknowledgements

The presented work is part of the EMPIR EURAMET-founded joint research project no. 17NRM03 “Standards for the evaluation of the uncertainty of coordinate measurements in industry EUCoM” coordinated by Alessandro Balsamo, INRIM.

## References

- [1] International Organization for Standardization. (2013). *Geometrical product specifications (GPS) – Coordinate measuring machines (CMM): Technique for determining the uncertainty of measurement – Part 1: Overview and metrological characteristics* (ISO/TS 15530-1:2013). <https://www.iso.org/obp/ui/#iso:std:iso:ts:15530:-1:ed-1:v1:en>.
- [2] Joint Committee for Guides in Metrology. (2009). *Evaluation of measurement data – An introduction to the “Guide to the Expression of Uncertainty in Measurement” and related documents* (JCGM 104:2009). [https://www.bipm.org/utils/common/documents/jcgm/JCGM\\_104\\_2009\\_E.pdf](https://www.bipm.org/utils/common/documents/jcgm/JCGM_104_2009_E.pdf).
- [3] Štrbac, B., Radlovački, V., Spasić-Jokić, V., Deliće, M., & Hadžistević, M. (2017). The difference between GUM and ISO/TC 15530-3 method to evaluate the measurement uncertainty of flatness by a CMM. *MAPAN*, 32(4), 251–257. <https://doi.org/10.1007/s12647-017-0227-3>
- [4] Płowucha, W., & Jakubiec, W. (2012). Proposal for changes in the ISO 15530 series of standards. *Calitatea*, 13(5), 237–240. <https://search.proquest.com/docview/1261387520?accountid=14903>.
- [5] Trapet, E., Savio, E., & De Chiffre, L. (2004). New advances in traceability of CMMs for almost the entire range of industrial dimensional metrology needs. *CIRP Annals*, 53(1), 433–438. [https://doi.org/10.1016/S0007-8506\(07\)60733-1](https://doi.org/10.1016/S0007-8506(07)60733-1)

- [6] Wilhelm, R. G., Hocken, R., & Schwenke, H. (2001). Task specific uncertainty in coordinate measurement. *CIRP Annals*, 50(2), 553–563. [https://doi.org/10.1016/S0007-8506\(07\)62995-3](https://doi.org/10.1016/S0007-8506(07)62995-3)
- [7] Verlag des Vereins Deutscher Ingenieure. (2011). Accuracy of coordinate measuring machines. Characteristics and their checking. Determination of the uncertainty of measurement for coordinate measuring machines using uncertainty budgets (VDI/VDE 2617-11:2011).
- [8] Pressel, H. G. & Hageney, T. (2008). *Messunsicherheit von Prüfmerkmalen in der Koordinatenmesstechnik*. Expert Verlag. (in German).
- [9] Hernla, M. (2014). *Messunsicherheit bei Koordinatenmessungen Abschätzung der aufgabenspezifischen Messunsicherheit mit Hilfe von Berechnungstabellen* (3rd ed.). Expert Verlag. (in German).
- [10] Mutilba U., Sandá A., Vega I., Gomez-Acedo E., Bengoetxea I., & Yagüe Fabra J. A. (2019). Traceability of on-machine tool measurement: Uncertainty budget assessment on shop floor conditions. *Measurement*, 135, 180–188. <https://doi.org/10.1016/j.measurement.2018.11.042>
- [11] Cheng, Y., Wang, Z., Chen, X., Li, Y., Li, H., Li, H., & Wang, H. (2019). Evaluation and optimization of task-oriented measurement uncertainty for coordinate measuring machines based on geometrical product specifications. *Applied Sciences*, 9(1). <https://doi.org/10.3390/app9010006>
- [12] Śladek J. A. (2016). Coordinate Metrology. Accuracy of Systems and Measurements. Springer-Verlag Berlin Heidelberg. <https://doi.org/10.1007/978-3-662-48465-4>
- [13] Jakubiec, W., Płowucha, W., & Starczak, M. (2012). Analytical estimation of coordinate measurement uncertainty. *Measurement*, 45(10), 2299–2308. <https://doi.org/10.1016/j.measurement.2011.09.027>
- [14] Arenhart, F. A., Donatelli, G. D., & Porath, M. C. (2012). An experimental method for assessing the contribution of the production process variations to the task-specific uncertainty of coordinate measurements. *Measurement*, 45(3), 507–516. <https://doi.org/10.1016/j.measurement.2011.10.021>
- [15] Forbes, A. (2018). Uncertainties associated with position, size and shape for point cloud data. *Journal of Physics: Conference Series*, 1065(14). <https://doi.org/10.1088/1742-6596/1065/14/142023>
- [16] Heisselmann, D., Franke, M., Rost, K., Wendt, K., Kistner, T., & Schwehn, C. (2017). Determination of measurement uncertainty by Monte Carlo simulation. In Forbes, A. B., Chunovkina, A.G., Eichstadt, S., Zhang, N. F., & Pavese, F. (Eds.). *Advanced Mathematical and Computational Tools in Metrology and Testing XI*, 89, (pp. 192–202). World Scientific. [https://doi.org/10.1142/9789813274303\\_0017](https://doi.org/10.1142/9789813274303_0017)
- [17] Li, H., Chen, X., Cheng, Y., Liu, H., Wang, H., Cheng, Z., & Wang, H. (2017). Uncertainty Modeling and Evaluation of CMM Task Oriented Measurement Based on SVCMM. *Measurement Science Review*, 17(5). <https://doi.org/10.1515/msr-2017-0027>
- [18] Płowucha, W. (2019). Point-straight line distance as model for uncertainty evaluation of coordinate measurement. *Measurement*, 135, 83–95. <https://doi.org/10.1016/j.measurement.2018.11.008>
- [19] International Organization for Standardization. (2006). *Statistics – Vocabulary and symbols – Part 1: General statistical terms and terms used in probability* (ISO 3534-1:2006). <https://www.iso.org/standard/40145.html>
- [20] International Organization for Standardization. (2009). *Geometrical product specifications (GPS) – Acceptance and reverification tests for coordinate measuring machines (CMM) – Part 2: CMMs used for measuring linear dimensions* (ISO 10360-2:2009). <https://www.iso.org/standard/40954.html>
- [21] International Organization for Standardization. (2011). *Geometrical product specifications (GPS) – Inspection by measurement of workpieces and measuring equipment – Part 2: Guidance for the estimation of uncertainty in GPS measurement, in calibration of measuring equipment and in product verification* (ISO 14253-2:2011). <https://www.iso.org/standard/53631.html>
- [22] Gromczak, K., Ostrowska, K., Owczarek, D., & Śladek, J. (2015). Validation of the metrological model of coordinate measuring arm using multifeature check. *Advances in Science and Technology Research Journal*, 9(27), 120–124, <https://doi.org/10.12913/22998624/60798>



**Wojciech Płowucha** received the Ph.D. degree from the University of Bielsko-Biała, Poland, in 2006. He is currently an Associate Professor at the Laboratory of Metrology of the University of Bielsko-Biała. His current research interests include GPS, measurement uncertainty of coordinate measurements. He took part in 6 EU-funded projects (including 3 as coordinator) concerning metrology education. Currently, he participates in another EMPIR-funded research project no. 17NRM03 “EUCoM” as

the leader of the UBB team.